*Thermochimica Acta*, 232 (1994) 7–18
Elsevier Science B.V., Amsterdam
*SSDI* 0040-6031(93)01382-D



# Thermal transition of plasmid pBR322 closed circular, open circular and linear DNAs

Hatsuho Uedaira *[a], Shun-ichi Kidokoro [b], Satoru Ohgiya [c], Kozo Ishizaki [c] and Nariko Shinriki [c]

[a] *National Institute of Bioscience and Human Technology, Tsukuba, Ibaraki 305 (Japan)*
[b] *Sagami Chemical Research Center, Sagamihara, Kanagawa 229 (Japan)*
[c] *Government Industrial Development Laboratory, Hokkaido, Toyohira, Sapporo 062 (Japan)*

(Received 24 May 1993; accepted 2 June 1993)

**Abstract**

Thermal transitions of pBR322 closed circular (cc), open circular (oc) and linear (l) DNAs have been measured by calorimetry. Six or eight peaks were observed for l and oc DNAs in 0.1× SSC and 1× SSC buffer solutions in the temperature ranges 67–84°C and 82–97°C, respectively, while ccDNA showed one broad peak at 103°C. Thermal reversibility was excellent for lDNA and good for ocDNA but the DSC curve of ccDNA at the consequent second heating was quite different from that of the first run. The morphological changes induced by heating cc and ocDNAs have been examined by electrophoresis of the preheated samples. ccDNA which was heated above 75°C was found to be converted partly to ocDNA, the amount of ocDNA increasing with increasing temperature. The DSC curve of lDNA in 0.1× SSC has been deconvoluted to a 24-state transition, and thermodynamic functions for the multistep transitions have been estimated; the results are discussed in comparison with its theoretical melting curve and its genetic map.

## INTRODUCTION

The morphological change from supercoiled plasmid pBR322 DNA (ccDNA) to open circular DNA (ocDNA) has been found to occur with the strand scission of ccDNA by the reaction of a chemical reagent such as ozone [1, 2] and by mung bean nuclease [3]. The position of cleavage has been discussed in relation to the regional AT-content and loop structure of ccDNA [1, 2]. The supercoiled plasmid ccDNA, in which the double-stranded helical DNA is twisted, is found to be more stable against heat or degradation by ultraviolet light than linear DNA (lDNA) and ocDNA

* Corresponding author.

[4, 5]. In order to elucidate further the effect of heating on these morphologically different forms of DNA, it is necessary to measure precisely by microcalorimetry their their thermodynamic properties, such as thermal transition temperature, enthalpy and reversibility, using highly purified samples of cc, oc and lDNA.

The blockwise and co-operative multistep thermal transition of double-stranded linear DNA from helix to coil has been studied by spectroscopic and microscopic methods and the algorithms for the calculation of the melting profile have been investigated [6–15]. Recently, Maeda et al. reported the multistep melting fine structure of linear plasmid pJL3-TB5, its derivatives [16–18] and ColE1 plasmid DNA [19] by calorimetry. The correlations between thermal melting profiles of DNAs and their biological functions have been statistically examined [7, 11–14, 19, 20]. Although the thermodynamic properties of the thermal transition for each of these steps are indispensable for a quantitative understanding of the helical fine structure of DNAs, the precise deconvolution analysis of direct thermodynamic measurements has not yet been carried out.

In this paper, we report the thermal transition of pBR322 cc. oc and lDNAs obtained from *Escherichia coli* HB101 measured by adiabatic differential scanning calorimetry (DSC) and electrophoresis. The difference in the thermal transitions of these three forms of DNA has been clarified. The experimental calorimetric melting curve for lDNA has been deconvoluted and thermodynamic functions for the multistep transitions are calculated. The results are discussed in comparison with its theoretical melting curve, its genetic map and the base pair positions which correspond to the weakest regions of ccDNA against cleavage by ozone.

## EXPERIMENTAL

### *Materials and preparation of plasmid pBR322 DNAs*

Mung bean nuclease and restriction endonuclease EcoRI were purchased from Tanaka Shuzo Co. Agarose for gel electrophoresis was obtained from Sigma Chemical Co. and TOYOPEARL HW-75S gel from Toyo Soda Manufacturing Co. Ltd. The plasmid was prepared from *Escherichia coli* strain HB101 transformant harboring plasmid pBR322 DNA according to a reported procedure of Norgard [21]. For the purification of ccDNA, the plasmid was subjected to gel chromatography using TOYOPEARL HW-75S as previously reported [22]. In order to obtain ocDNA with the least number of nicks, we modified the conditions for hydrolysis of ccDNA proposed by Kowalski [3] as follows: 500 g of pure ccDNA was dissolved in 0.5 ml of 10 mM Tris-HCl buffer (pH 7.5). After preincubation for 15 min at 47°C, a 138U aliquot of mung bean nuclease was added and kept at 47°C

for 30 min. The ocDNA produced was purified as usual. lDNA was prepared by digestion of pure ccDNA with restriction endonuclease EcoRI and purified. The purity of both ocDNA and lDNA was confirmed by gel electrophoresis. Ethanol–NaCl solutions which contained 0.9 mg portions of DNA were stored in microtubes at −30°C.

*Differential scanning calorimetry and deconvolution of the DSC data*

1× SSC and 0.1× SSC buffer solutions (SSC is 0.15 M NaCl, 0.015 M sodium citrate, pH 7.0) were used for the measurement of thermal transition of DNAs by DSC and electrophoresis. DNAs were recovered from ethanol–NaCl solutions by centrifugation, dried and dissolved in sterilized SSC buffer solutions. All the vessels, pipettes and calorimetric cells used were sterilized. The concentration of DNAs for calorimetry was 0.67 mg $ml^{-1}$. The calorimetric measurements were made on a differential scanning microcalorimeter DASM-1M [23] at a heating rate of 0.5°C $min^{-1}$ under an excess pressure of 1.1 bar in calorimeter cells. The DSC data were acquired every 2 s using a PC9801 personal computer [24]. For sufficient cooling of the solutions in calorimeter cells, the usual time interval between the end of a DSC run and the beginning of the next reheating run was about 100 min.

The thermal transition curve of lDNA in 0.1× SSC buffer solution was analyzed by the deconvolution based on previously reported method [25, 26]. In analysis it was assumed that the double stranded DNA helix is dissociated into two DNA molecules at the final thermal transition step, and that at the DNA concentrations of our experiments, the heat capacity difference of DNA between native and thermally denatured states is zero. Using about 540 data points, the initial parameter set was obtained by the single and double deconvolution methods on an NEC 9801 microcomputer and was further adjusted by a non-linear least squares fitting method [26] using the program SALS [27] on a FACOM M780 computer. The enthalpy change of each transition is estimated as the difference from the enthalpy of the consequent former state.

*Examination of heat-treated DNAs by electrophoresis*

To examine the changes of ccDNA and ocDNA by heating, the microtubes containing 40 $\mu$l of DNA solution of 0.1× SSC buffer solution (0.25 g $\mu l^{-1}$) were tightly plugged and heated to various temperatures in an incubator at a heating rate of 1°C $min^{-1}$. Microtubes which were taken from the incubator were slowly cooled and kept at 4°C. These DNAs were precipitated by ethanol–NaCl, stored at −30°C, and were recovered by centrifugation before use as described above. The DNA was subjected to 1% agarose gel electrophoresis [22].

*Calculation of theoretical melting profiles, denaturation maps and thermal stability maps*

The theoretical calculations for lDNA in 0.1× SSC buffer solution was made using the nucleotide sequence of pBR322 (4362 base pairs). Theoretical melting curves and denaturation maps were calculated according to the algorithms for the "base-pair model" by Poland [28] and Fixman and Freire [29].

For the calculation of the melting in 0.1× SSC buffer solution, the following parameters [30] were used: $T_{AT} = 53.1°C$, $T_{GC} = 94.1°C$ and $\Delta S = -24.54$ e.u., where $T_i$ is the temperature of helix-to-coil transition for base-pair $i$, and $\Delta S$ is the entropy decrease in pairing per base pair. The values of $T_{AT}$ for the Dam site in which adenine in the sequence GATC is methylated was assumed to be lower than 53.1°C. The helix-to-coil stability factor $r_i$ for the $i$th base-pair is

$$r_i = \exp\{-(\Delta H_i - T\Delta S)/RT\}$$

The values for the loop entropy factor $\sigma_n$, and concentration dependency factor, $\beta C_0$ [30,31], are $\sigma_n = 6 \times 10^{-6}(n + 450)^{-1.75}$ and $\beta C_0 = 1 \times 10^{-7}$, where $n$ denotes the numbers of unbonded base pairs included in an internal loop. The theoretical melting profile and the thermal stability map were calculated using the computer program kindly supplied by Suyama [32].

## RESULTS AND DISCUSSION

*Thermal transition of l, oc and ccDNA*

DSC curves for the thermal transition of lDNA and ocDNA in 0.1× SSC and 1× SSC buffer solutions are shown in Figs. 1 and 2, respectively. The

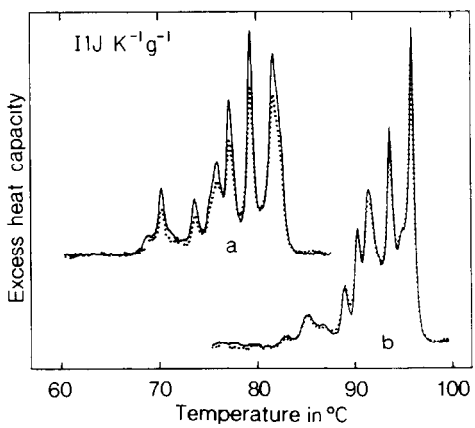


Fig. 1. Heat capacity curves of lDNA in 0.1× SSC (curve a) and 1× SSC (curve b) buffer solutions. Solid and dotted lines denote first and second runs, respectively.

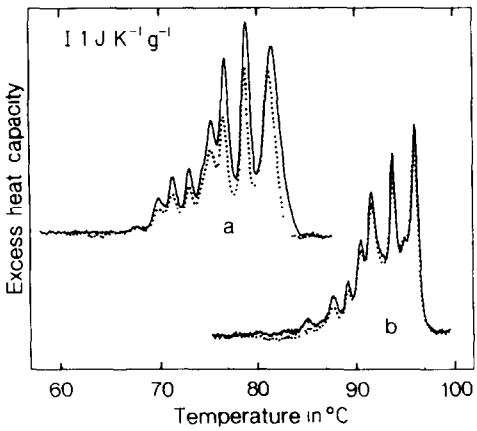


Fig. 2. Heat capacity curves of ocDNA in 0.1× SSC (curve a) and 1× SSC (curve b) buffer solutions. Solid and dotted lines denote first and second runs, respectively.

solid curves are the transition curves for the first run and dotted curves denote the transition at the second heating. Six or seven peaks with shoulders are observed for l and ocDNAs, respectively. The transitions of both l and ocDNAs in 0.1 and 1× SSC buffer solutions are observed in the temperature ranges 67–84°C and 82–97°C, respectively. The melting temperatures of these peaks in 1× SSC solution are 13–15°C higher than those in 0.1× SSC buffer solution, which shows that increase in ionic strength stabilizes DNAs in accordance with the results of Perelroyzen et al. [33] and Wada and Suyama [14]. The shapes of the three peaks at higher temperature for lDNA and ocDNA resemble each other. The difference in the shape of DSC curves at lower temperature between ocDNA and lDNA seems to be due to the ring structure of ocDNA.

The agreement of the curves for the first and second runs indicates that the reversibility of the thermal transition of lDNA in both buffer solutions is excellent and that of ocDNA is good. To examine the effect of heating on DSC curves of ocDNA for the first and second runs, gel electrophoresis measurements were made on heat-treated ocDNA in 0.1× SSC buffer solutions, and the results are shown in Fig. 3. ocDNA was not changed up to 75°C, but at temperatures higher than 85°C, a small amount of lDNA and faint smear bands appeared. The heat induced breakage of ocDNA does not affect the DSC curve in the first run, as the thermal denaturation of ocDNA in 0.1× SSC buffer solution is completed at 84°C. The effect of brekage, however, seems to cause a small difference in the second run of ocDNA in the DSC measurements. The highest DSC peak for the second run of ocDNA in 0.1× SSC buffer solution closely resembles that of the corresponding highest peak of lDNA, supporting the electrophoresis results. The good reversibility of the thermal denaturation of ocDNA in 1× SSC buffer solution was supported by the results of gel electrophoresis

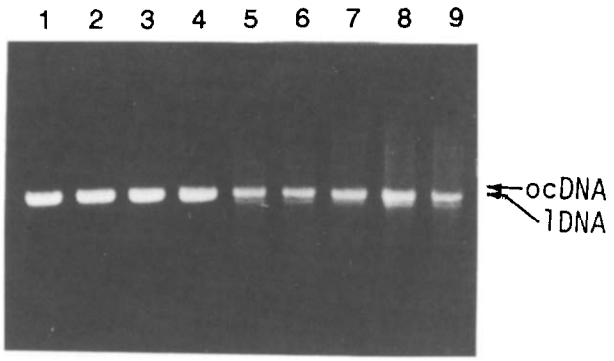


Fig. 3. The effect of heat treatment on ocDNA in 0.1× SSC buffer solutions. Samples of ocDNA solutions were heated at a rate of 1° $min^{-1}$ up to various temperatures: 1, untreated; 2, 55°C; 3, 65°C; 4, 75°C; 5, 85°C; 6, 88°C; 7, 91°C; 8, 94°C; 9, 97°C.

which show that ocDNA does not change upon heating up to 97°C (data not shown). As it is difficult to calculate the energy of distortion of the DNA chain in ocDNA, further precise analysis of the thermal transition for ocDNA was not made, but the DSC curves show that fine transitional structure in ocDNA is not greatly different from that of lDNA.

The thermal transition of ccDNA in 0.1× SSC buffer solutions was measured repeatedly and the results are shown in Fig. 4. In the first run, one broad peak with maximum heat capacity at 103°C was observed. As shown in the figure, the DSC curve for the second run is quite different from that of the first, but is in accord with the pattern of ocDNA. To confirm the appearance of ocDNA upon heat treatment of ccDNA, heat-treated ccDNA in 0.1× SSC buffer solution was examined by electrophoresis.

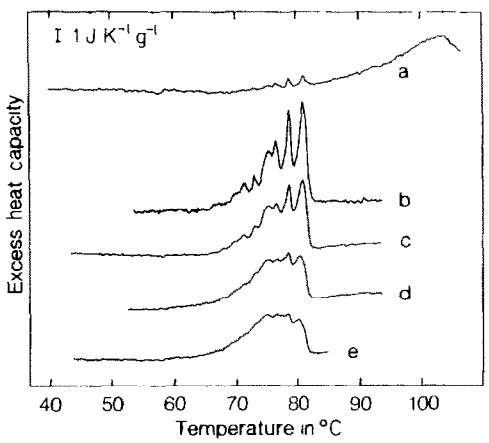


Fig. 4. Heat capacity curves of ccDNA in 0.1× SSC buffer solution obtained by repeated calorimetric scan. Curves a, b, c, d and e denote DSC curve at 1st, 2nd, 3rd, 5th and 7th run, respectively.

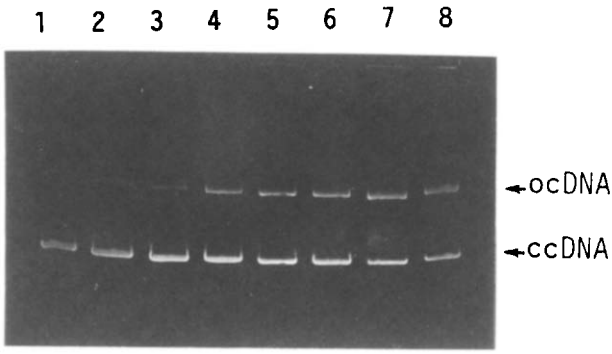


Fig. 5. The effect of heat treatment on the morphological change of ccDNA in 0.1× SSC buffer solutions. ccDNA solutions were heated at a heating rate of 1°C $min^{-1}$ up to various temperatures: 1, untreated; 2, 65°C; 3, 75°C; 4, 85°C; 5, 90°C; 6, 94°C; 7, 96°C; 8, 98°C.

Figure 5 shows that a small amount of ocDNA appeared at 75°C, and above 85°C the amount of ocDNA increased gradually with increase in temperature. In the DSC curve for the first run of ccDNA, the small peaks around 80°C are considered to be due to the small amount of ocDNA produced by heating ccDNA. Above 85°C, even if ocDNA is present, it is already in the denatured satate as shown in Fig. 2 and cannot affect the heat capacity curve; consequently, the broad peak at 103°C is considered to be due to gradual scission followed by denaturation of the remaining small amount of ccDNA.

After the repeated heat treatment of ccDNA, although the transition temperature range is not changed, the clear peaks in the second run became obscure, and the DSC curve at the seventh run shows a very broad peak. The electrophoretic pattern for ccDNA recovered from a calorimetry cell after repeating the DSC measurements in 0.1× SSC buffer solution seven times showed broad bands of DNAs with smaller molecular weight than that of the initial ccDNA. The disappearance of the fine structural melting pattern after repeated runs, as shown in Fig. 4, is caused by the degradation of ocDNA which was observed at the second run.

The DSC curves of l and ocDNA (Figs. 1 and 2, respectively) show that the heat capacities of the native and denatured states for these DNAs are almost equal. That is, the heat capacity increase on denaturation $\Delta C_p$, which is usually observed in the case of thermal transition of proteins [34], is zero. To estimate the total enthalpy change of three types of DNA, the heat capacity curves of l and ocDNA in 0.1× SSC buffer solutions were integrated on the basis of heat capacities of the native states, and the values of 141 and 193 MJ $mol^{-1}$, respectively, were obtained. In the case of ccDNA, the heat capacity curve does not return to the baseline even at the highest temperature of 105°C which is measurable with the DASM-1M differential scanning microcalorimeter. Consequently, the precise value of

the enthalpy change cannot be obtained, but extrapolating the DSC curve at the native state and the DSC melting curve give a value between 200 and 220 MJ $mol^{-1}$. The enthalpy change for lDNA corresponds to the transition of the double helix to two monomeric random DNA molecules. The larger values of enthalpy change for oc and ccDNA compared with lDNA having the same base pair sequence are considered to be due to the energy of restriction of supercoiled forms and also the scission of main chains in the case of ocDNA and especially of ccDNA.

*Deconvolution of DSC curves for lDNA and comparison with data obtained by UV measurements*

The dotted line in Fig. 6(a) denotes the thinned out experimental molar heat capacity data (first run, total 550 points) of lDNA in 0.1× SSC buffer solution. The DSC curve which has six peaks with shoulders clearly demonstrates that the thermal transition of lDNA is a multistate transition. In order to clarify further whether the observed six peaks are due to two-state transitions or not, the DSC curve was analyzed by the single and double deconvolution methods [26]. The results shows that these peaks can be decomposed into 23 transitions, which means that each peak observed in a DSC curve is composed of between three and six transitions. The obtained parameter set adjusted by the non-linear least squares method is

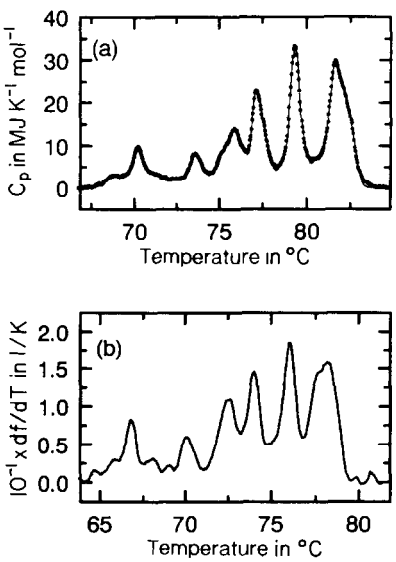


Fig. 6. Thermal transition curves of pBR322 plasmid lDNA in 0.1× SSC buffer solutions: (a) dotted and solid lines denotes experimental and calculated heat capacity curves, respectively; (b) differential profiles of melting obtained from UV measurement at 260 nm at a heating rate of 0.2°C $min^{-1}$ (data from Suyama [36]).

TABLE 1

Transition temperature and enthalpies for 24-state transition of plasmid pBR322 lDNA in a 0.1× SSC buffer solution

| No. | Temperature/°C | Enthalpy/kJ $mol^{-1}$ |
|---|---|---|
| 1 | 68.81 ± 0.02 | 3353 ± 70 |
| 2 | 69.97 ± 0.03 | 3890 ± 130 |
| 3 | 70.32 ± 0.02 | 4630 ± 130 |
| 4 | 71.28 ± 0.03 | 3524 ± 70 |
| 5 | 72.72 ± 0.04 | 3030 ± 72 |
| 6 | 73.63 ± 0.01 | 5395 ± 63 |
| 7 | 74.55 ± 0.03 | 3764 ± 69 |
| 8 | 75.30 ± 0.01 | 5707 ± 63 |
| 9 | 75.84 ± 0.01 | 6755 ± 59 |
| 10 | 76.37 ± 0.01 | 5880 ± 58 |
| 11 | 77.02 ± 0.004 | 7895 ± 73 |
| 12 | 77.35 ± 0.01 | 7391 ± 69 |
| 13 | 77.78 ± 0.01 | 5774 ± 72 |
| 14 | 78.72 ± 0.01 | 5219 ± 71 |
| 15 | 79.16 ± 0.004 | 8851 ± 76 |
| 16 | 79.44 ± 0.004 | 8997 ± 75 |
| 17 | 79.81 ± 0.01 | 6205 ± 74 |
| 18 | 80.59 ± 0.01 | 5329 ± 59 |
| 19 | 81.24 ± 0.01 | 7235 ± 72 |
| 20 | 81.58 ± 0.004 | 9175 ± 74 |
| 21 | 81.90 ± 0.01 | 8466 ± 74 |
| 22 | 82.29 ± 0.01 | 7087 ± 77 |
| 23 | 82.68 ± 0.01 | 7704 ± 99 |

shown in Table 1. The solid line in Fig. 6(a) denotes the calculated heat capacity curve based on these parameters, with the residual mean square deviation between calculated and experimental heat capacity of 0.5 MJ $K^{-1}$ $mol^{-1}$. Although there is no other method to confirm whether or not the thermal transition of lDNA is exactly a 23-state transition (because there is no other method by which such multistate transitions can be energetically analyzed) the calorimetric data is excellently fitted by thermodynamic functions with 23 transitions.

In Table 1, transitions numbered 1–4, 5–7, 8–10, 11–13, 14–17 and 18–23 corresponds, respectively, to peaks 1–6 in Fig. 6. The average enthalpy values for the transitions which are included in these six peaks are 3850, 4060, 6110, 7020, 7320 and 7500 kJ $mol^{-1}$, respectively. Generally speaking, the cooperative melting regions at higher temperature melt with higher enthalpy change.

The thermal melting curve calculated from the UV measurements of pBR322 plasmid lDNA by Suyama [36] is shown in Fig. 6(b), which is similar to but a little different from that measured by Perelroyzen et al.

[33]. Figure 6 strongly demonstrates that the agreement of the shape of the melting curve between DSC and UV measurements is excellent. The fact that the denaturation temperature observed by UV measurement is lower than that observed by DSC by about 4°C may be caused by the difference of the concentration of lDNA, that is, by the difference in ionic strength in these measurements.

*Theoretical melting curves, thermal stability map and relation to biological functions of lDNA*

To correlate the thermodynamic data with the base number, the theoretical melting curve of lDNA, which is the differential of the decrease in the native fraction, was calculated by Suyama and Wada's program [32] using the nucleotide sequence data of pBR322, and is plotted against temperature in Fig. 7(a). The melting curves with various $T_{AT}$ values for

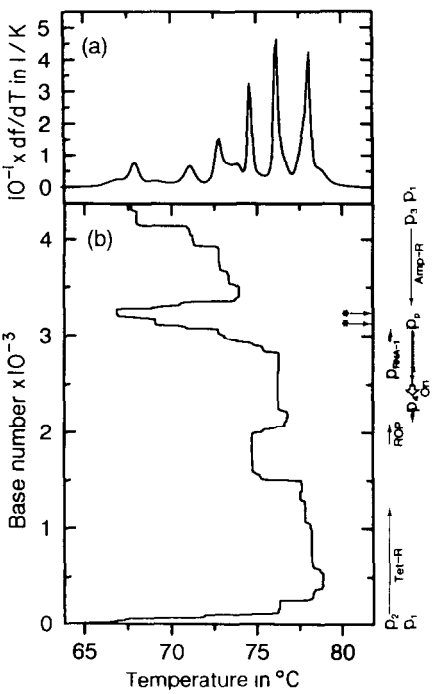


Fig. 7. A thermal stability map (a) and a calculated melting profile with a gene map (b) for pBR322 plasmid lDNA. Straight arrows represent protein-coding regions for ampicillin-resistance, tetracycline-resistance and ROP. Promoters for these genes are $P_1$ and $P_3$, $P_2$, and an unknown which should be before the ROP gene, respectively. Wavy arrows represent RNA transcripts for the RNA primer for DNA replication and RNA-1. Promoters for these RNAs are $P_p$ and $P_{RNA-1}$, respectively. $P_4$ is a promoter activated by cyclic AMP receptor protein in vitro. Ori represents origin of replication of pBR322 DNA. The asterisk represents the ozone-sensitive S1 sites confirmed by us [1, 2].

Dam sites were checked in comparison with experimental melting curves obtained by calorimetry and spectroscopy; it was found that the curve with $T_{AT} = 0°C$ for the Dam site most properly predicts the experimental melting curves. The melting temperature of the theoretical curve is about 3–4°C lower than the experimental curve obtained by calorimetry and coincides with the curve given by UV measurements. The thermal stability map of pBR322 DNA in 0.1× SSC buffer solution along with its genetic map is also shown (Fig. 7(b)). The abscissa is the melting temperature of each base pair. The complexity of the melting curve in Fig. 7 indicates it is reasonable that each melting peak has more than three transitions with different mid-point temperatures.

By comparing the thermal stability map with the DSC curve, each peak in the DSC curve can be assigned to the base pairs in the DNA sequence. Peaks 1 and 2 with the lowest melting temperatures in Fig. 6 correspond to the calculated transition at 66–73°C in Fig. 7(a), which is due to the melting of bases at numbers 3050–3350 and terminal regions, as shown in Fig. 7(b). The promoter for the RNA primer of DNA replication ($P_p$), and promoters $P_1$, $P_2$ and $P_3$ are located in these regions [35]. The S1 sites (3120bp and 3220bp) which were confirmed to be ozone-sensitive by us [1, 2] and seven methylated adenines among the total 22 GATC sequences having methylated adenines are also located in this region. These regions are biologically active and melt at the lowest temperature ranges with the smallest average values of $\Delta H$ of about 3850 and 4060 kJ mol$^{-1}$.

The straight arrow region, which represents the protein coding region for ampicillin-resistant protein (Amp-R), a region of base pair numbers 3400–3900, belongs to the third peak of the DSC curve in Fig. 6, and melts with average enthalpy change of 6100 kJ mol$^{-1}$.

The fourth peak, with an average enthalpy change of 7020 kJ mol$^{-1}$ is caused by melting of the regions of base pair numbers 1530–2050 and 2850–2950; it is deconvoluted to three transitions. Replication origin (Ori) is located at base pairs between 2050 and 2850 with an average enthalpy change of 7300 kJ mol$^{-1}$ (fifth peak). The most thermally stable part between base pairs 400 and 600, in which the GC content is as high as 65%, is included in the protein coding region of tetracycline-resistance (Tet-R), which melts with the highest average enthalpy changes of 7500 kJ mol$^{-1}$.

ACKNOWLEDGMENTS

We thank Drs A. Wada (Sagami Chemical Research Center) and A. Suyama (University of Tokyo) for kindly offering the computer program and allowing us to use their unpublished melting curve data obtained by UV measurements and shown in Fig. 6(b). We are grateful to Dr Y. Maeda (Iwaki Myoujou University) for valuable suggestions about the effect of Dam sites on the theoretical melting curve.

## REFERENCES


1 K. Sawadaishi, K. Miura, T. Ohtsuka, T. Ueda, K. Ishizaki and N. Shinriki, Nucleic Acids Res., 13 (1985) 7183–7194.
2 K. Sawadaishi, K. Miura, E. Ohtsuka, T. Ueda, K. Ishizaki and N. Shinriki, Nucleic Acids Res., 14 (1986) 1159–1168.
3 L.G. Sheflin and D. Kowalski, Nucleic Acids Res., 13 (1985) 6137–6154.
4 D. Freifelder, P.F. Dadison and E.P. Geiduschek, Biophys. J., 1 (1961) 389–400.
5 J. Vinograd and J. Lebowits, J. Gen. Physiol., 49 (1966) 103–125.
6 G. Bernrdi, M. Faures, G. Piperno and P.P. Slonimski, J. Mol. Biol., 48 (1970) 23–42.
7 S. Yabuki, M. Fuke and A. Wada, J. Biochem., 69 (1971) 191–207.
8 A.S. Borovik, Yu. A. Kalambet, Yu. L. Lyubchenko, V.T. Shitov and Vu.I. Golovanov, Nucleic Acids Res., 8 (1980) 4165–4185.
9 A. Wada, S. Yabuki and Y. Hushimi, CRC Crit. Rev. Biochm., 9 (1980) 87–144.
10 R.D. Wells, T.C. Goodman, W. Hilleu, G.T. Horn, R.D. Klein, L.E. Larson, U.R. Muller, S.K. Neuendorf, N. Danayotatos and S.M. Stirdivant, Prog. Nucleic Acid Res. Mol. Biol., 24 (1980) 168–267.
11 O. Gotoh, Adv. Biophys., 16 (1983) 1–52.
12 A. Suyama and A. Wada, J. Theor. Biol., 105 (1983) 133–145.
13 R.M. Wartell and A.S. Benight, Phys. Rep., 126 (1985) 67–107.
14 A. Wada and A. Suyama, Prog. Biophys. Mol. Biol., 47 (1985) 113–157.
15 R.D. Blake and S.G. Delcourt, Biopolymers, 26 (1987) 2009–2026.
16 Y. Maeda, Y. Kawai, T. Fujita and E. Ohtsubo, J. Gen. Appl. Microbiol., 30 (1984) 289–295.
17 Y. Maeda, Y. Kawai, T. Fujita and E. Ohtsubo, Thermochim. Acta, 88 (1985) 235–240.
18 Y. Maeda and E. Ohtsubo, J. Mol. Biol., 194 (1987) 691–698.
19 Y. Maeda, K. Takahashi, H. Yamaki and E. Ohtsubo, Biopolymers, 27 (1988) 1917–1925.
20 H. Yamaki, E. Ohtsubo, K. Nagai and Y. Maeda, Nucleic Acids Res., 16 (1988) 5067–5073.
21 M.V. Norgard, Anal. Biochem., 113 (1981) 34–42.
22 K. Ishizaki, K. Sawadaishi, K. Miura and N. Shinriki, Water Res., 21 (1981) 823–827.
23 P.L. Privalov, Pure Appl. Chem., 52 (1980) 479–497.
24 H. Uedaira and S. Kidokoro, Thermochim. Acta, 183 (1991) 323–328.
25 S. Kidokoro and A. Wada, Biopolymers, 26 (1987) 213–226.
26 S. Kidokoro, H. Uedaira and A. Wada, Bipolymers, 27 (1988) 271–297.
27 T. Nagasawa and Y. Oyanagi, in K. Matsusita (Ed.), Recent Developments in Statistical Influence and Data Analysis, North Holland, Amsterdam, 1989, pp. 221–225.
28 D. Poland, Biopolymers, 13 (1974) 1859–1871.
29 M. Fixman and J.J. Freire, Biopolymers, 20 (1977) 1033–1042.
30 Yu. L. Lyubchenko, A.V. Vologodoskii and M.D. Frank-Kamenetskii, Nature, 271 (1978) 28–31.
31 O. Gotoh and Y. Tagashita, Biopolymers, 20 (1981) 1033–1042.
32 A. Suyama and A. Wada, Biopolymers, 23 (1984) 409–433.
33 M.P. Perelroyzen, V.I. Lyamichev, Yu.A. Kalambet, Yu. L. Lyubchenko and A.V. Volgodskii, Nucleic Acids Res., 9 (1981) 4043–4059.
34 P.L. Privalov, Adv. Protein Chem., 33 (1979) 167–241.
35 D. Stuber and H. Bujard, Proc. Natl. Acad. Sci. USA, 78 (1981) 167–171.
36 A. Suyama, unpublished data.